Hyperpolarizabilities of alkali halide crystals using the local-density approximation

M. D. Johnson and K. R. Subbaswamy
Department of Physics and Astronomy, University of Kentucky, Lexington, Kentucky 40205-0055

G. Senatore
Dipartimento di Fisica Teoricabibre, Universita di Trieste, Trieste, Italy
(Received 27 April 1987)

Static electronic hyperpolarizabilities of alkali halide crystals are computed in a local-density-approximation scheme. It is found that the anion nonlinear susceptibilities are extremely sensitive to the crystalline environment while the cation values are not. Calculations using pseudopotentials to represent overlapping neighbors are found to yield very reasonable agreement with extrapolated experimental values.

I. INTRODUCTION

Nonlinear optical susceptibilities enter in the description of a variety of phenomena in solids, such as four-wave mixing,[1] third-harmonic generation,[1] coherent and hyper-Raman spectroscopy,[2] etc. Since the initial experiments[1] after the development of the laser, experimental techniques have steadily improved, and in some cases even the electronic and lattice contributions to nonlinear indices have been determined.[3] However, theoretical calculations of nonlinear susceptibilities have lagged behind.

With the development of increasingly reliable computational schemes, some nonlinear susceptibilities of rare-gas atoms have been computed recently using the local-density approximation[4,5] (LDA) and fourth-order many-body perturbation methods.[6] These calculations yield results at the level of semiquantitative to quantitative agreement with experiments. For crystalline solids, however, the calculations have been limited to simplified bond-charge models,[7] with a notable exception.[8] Recently, there has been a cluster-type calculation of the hyperpolarizability of LiF and LiCl within the many-body perturbation scheme.[9]

The purpose of this paper is to describe an LDA calculation of the static electronic hyperpolarizabilities of alkali halide crystals and compare them with experimental results. Since experimental measurements of nonlinear susceptibilities of alkali halides are rather scarce, it is our hope that our calculations will stimulate further experiments. The calculations presented here are also a first step towards an extensive treatment of nonlinear susceptibilities and polarizability derivatives of insulators and semiconductors which we are undertaking.

The use of LDA to describe anions needs some justification. It is well known that free anions are predicted to be unbound in LDA,[10] unless one makes corrections for self-interactions. It is also known that if the extra electron is confined to a region near the atom, LDA gives reasonable binding energies for anions.[11] In ionic crystals the Madelung potential confines the extra electron to the vicinity of the anion nucleus, giving rise to binding even without self-interaction correction (SIC). In fact, Jansen and Freeman[12] have recently reported excellent ground-state properties for NaCl using LDA. Also, Mahan[16] has reported excellent values for the linear polarizabilities of alkali halide crystals using LDA. One can argue that in light of the Madelung and overlap potentials in the crystal, SIC should have a minor effect. We have shown earlier[4] that the usual SIC schemes are not satisfactory for the polarizability calculation. For these reasons, we have used the LDA in our calculations.

The nonlinear susceptibilities addressed in this paper may be introduced by writing the induced dipole and quadrupole moments of an atom or molecule in a uniform static external electric field $\mathbf{F}$ as[13]

$$p_\mu = \alpha_{\mu\nu}F_\nu + \frac{1}{3!}\gamma_{\mu\nu\delta\tau}F_\nu F_\delta F_\tau + \cdots , \tag{1}$$

$$q_{\alpha\beta} = \tfrac{1}{6}B_{\alpha\beta\mu\nu}F_\mu F_\nu + \cdots . \tag{2}$$

The tensor α is the linear dipole polarizability, and γ and B are, respectively, the dipole and quadrupole hyperpolarizabilities. In a cubic environment $\alpha_{\mu\nu}=\alpha\delta_{\mu\nu}$ and there are only two independent components of each of the tensors γ and B: γ_{zzzz}, γ_{xxzz}, B_{zzzz}, and B_{xzxz}. For a spherically symmetric environment one further has $\gamma_{xxzz}=\frac{1}{3}\gamma_{zzzz}$ and $B_{xzxz}=\frac{3}{4}B_{zzzz}$.

In Sec. II we describe the LDA calculation of polarizabilities. Section III contains an assessment of the calculational scheme and presents our results for the linear and nonlinear polarizabilities. In Sec. IV we compare the latter with experimental measurements, and, finally, Sec. V contains a summary of our conclusions.

II. METHOD OF CALCULATION

The LDA calculation of electronic hyperpolarizabilities presented here proceeds in two steps. First we compute an ion's ground-state electron density in zero field, and then find the density distortion induced by a per-

turbing electric field. The accuracy of this approach depends crucially on how well we represent the local environment of each ion, and towards this end we have tested two approaches: a completely self-consistent *ab initio* method,[14,4] where each ion in the crystal is treated on an equal footing, and a method of pseudopotentials,[15,16] in which all ions but one are represented by pseudopotentials. Both approaches are based on the Kohn-Sham formulation of density-functional theory.[17] These two methods are described in Secs. II A and II B, and finally in Sec. II C we summarize the LDA perturbative calculation of the polarizabilities.

A. Completely self-consistent method

The self-consistent density-functional-theory technique described here has been used for neutral closed-shell ions in isolation and in a crystal.[14,4] Here we sketch the calculation with emphasis on the changes needed for an ionic crystal consisting of two types of charged, closed-shell ions.

The total crystal energy can be written as a functional of the total electron density $n(\mathbf{r})$;[18] here it takes the form

$$E=T[n]+U_{e\text{-}n}[n]+U_H[n]+U_{\rm xc}[n]+U_{n\text{-}n} \ , \tag{3}$$

$$U_{e\text{-}n}=\int d^3r\, n(\mathbf{r})V_n(\mathbf{r}) \ , \tag{4}$$

$$V_n(\mathbf{r})=-2\sum_{\mathbf{R}}\frac{Z_{\mathbf{R}}}{|\mathbf{r}-\mathbf{R}|} \ , \tag{5}$$

$$U_H=\int d^3r\int d^3r'\frac{n(\mathbf{r})n(\mathbf{r}')}{|\mathbf{r}-\mathbf{r}'|} \ . \tag{6}$$

Above and throughout this paper we write energies in units of rydbergs ($e^2/2a_0$) and lengths in units of a_0 (the Bohr radius). $V_n(\mathbf{r})$ is the potential energy of an electron at $\mathbf{r}$ due to all of the nuclei; the ion at a site $\mathbf{R}$ has a nuclear charge $eZ_{\mathbf{R}}$. In (3) we have included the nuclear-nuclear electrostatic energy

$$U_{n\text{-}n}=\sum_{\mathbf{R}\neq\mathbf{R}'}\frac{Z_{\mathbf{R}}Z_{\mathbf{R}'}}{|\mathbf{R}-\mathbf{R}'|} \tag{7}$$

to keep the total energy finite. Nonetheless, $U_{n\text{-}n}$ is taken as fixed—the ions do not move. $U_{\rm xc}$ is the exchange-correlation energy and T the kinetic energy.

We assume[14] that the total electronic density can be written as a sum over contributions belonging to each ion:

$$n(\mathbf{r})=\sum_{\mathbf{R}}n_{\mathbf{R}}(\mathbf{r}-\mathbf{R}) \ , \tag{8}$$

where to begin with each ion is permitted a different density $n_{\mathbf{R}}$. Next, rewrite the kinetic energy as

$$\begin{aligned}T[n]&=\sum_{\mathbf{R}}T_s[n_{\mathbf{R}}]+\left[T[n]-\sum_{\mathbf{R}}T_s[n]\right]\\&\equiv\sum_{\mathbf{R}}T_s[n_{\mathbf{R}}]+U_K[n] \ ,\end{aligned} \tag{9}$$

where $T_s[n_{\mathbf{R}}]$ is the kinetic energy of the electronic density $n_{\mathbf{R}}$ in the absence of surrounding ions and U_K represents an unknown contribution from electron-electron overlap.

Now minimize E with respect to the electron density $n_{\mathbf{R}}$ at a particular site $\mathbf{R}$, while holding the remaining $n_{\mathbf{R}'}$ fixed. The result can be written in a Kohn-Sham form in which $n_{\mathbf{R}}$ is given as a sum over occupied orbitals $\psi_{\mathbf{R},\alpha}$ which satisfy a Schrödinger equation. The final step is to impose self-consistency: every cation is required to have the same density n_c and every anion the same density n_a. The result of this minimization–self-consistency procedure is that, placing an ion of type i [$i=a$ (anion) or c (cation)] at the center of coordinates,

$$n_{\mathbf{R}}(\mathbf{r})=n_i(\mathbf{r})=\sum_{\alpha(\rm occ)}|\psi_{i\alpha}(\mathbf{r})|^2 \quad (i=a,c) \ , \tag{10}$$

where the orbitals $\psi_{i\alpha}$ satisfy the Kohn-Sham equations

$$(-\nabla^2+V_{{\rm eff},i})\psi_{i\alpha}(\mathbf{r})=\varepsilon_{i\alpha}\psi_{i\alpha}(\mathbf{r}) \ , \tag{11}$$

$$\begin{aligned}V_{{\rm eff},i}(\mathbf{r})=&2\int\frac{d^3r'}{|\mathbf{r}-\mathbf{r}'|}\left[n_i(\mathbf{r}')+\sum_{\mathbf{R}\neq0}n_{\mathbf{R}}(\mathbf{r}'-\mathbf{R})\right]\\&-\frac{2Z_i}{r}-2\sum_{\mathbf{R}\neq0}\frac{Z_{\mathbf{R}}}{|\mathbf{r}-\mathbf{R}|}\\&+\frac{\delta U_{\rm xc}}{\delta n_i(\mathbf{r})}+\frac{\delta U_K}{\delta n_i(\mathbf{r})} \ .\end{aligned} \tag{12}$$

In the first approximation each ion surrounding a central ion can be replaced by a point charge I_i (±1 in the alkali halides), where

$$I_i=Z_i-\int d^3r\, n_i(\mathbf{r}) \quad (i=a,c) \ . \tag{13}$$

The contribution from these point charges, the Madelung potential, can formally be written

$$V_{\rm Mad}(\mathbf{r})=-2\sum_{\mathbf{R}\neq0}\frac{I_{\mathbf{R}}}{|\mathbf{r}-\mathbf{R}|} \ . \tag{14}$$

This sum converges poorly and it is physically sensible to separate out this contribution to (12). Doing so is equivalent to separating the ion at $\mathbf{R}$ into a point charge $I_{\mathbf{R}}$ plus a "neutralized" ion consisting of a nucleus of charge $Z_{\mathbf{R}}-I_{\mathbf{R}}$ surrounded by an electronic density $n_{\mathbf{R}}$. Then the effective potential (12) becomes, for a cation,

$$\begin{aligned}V_{{\rm eff},c}(\mathbf{r})=&2\int d^3r'\frac{n_c(\mathbf{r}')}{|\mathbf{r}-\mathbf{r}'|}-\frac{2Z_c}{r}+V_{{\rm Mad},c}+V_{{\rm xc},c}+V_{K,c}+\sum_{\substack{\mathbf{R}\neq0\\ \text{cations}}}\left[2\int d^3r'\frac{n_c(\mathbf{r}'-\mathbf{R})}{|\mathbf{r}-\mathbf{r}'|}-2\frac{Z_c-I_c}{|\mathbf{r}-\mathbf{R}|}\right]\\&+\sum_{\substack{\mathbf{R}\\ \text{anions}}}\left[2\int d^3r'\frac{n_a(\mathbf{r}'-\mathbf{R})}{|\mathbf{r}-\mathbf{r}'|}-2\frac{Z_a-I_a}{|\mathbf{r}-\mathbf{R}|}\right] \ ,\end{aligned} \tag{15}$$

with a similar expression for a central anion. In (15), $V_{\mathrm{Mad},c}$ is the Madelung potential (14) in coordinates chosen with a cation at the origin. We compute this (after spherically averaging, as discussed below) with a standard Ewald sum.

In self-consistently solving (11) with the effective potential [(15) and its anion analogue], several practical approximations are necessary. First is the local-density approximation for the exchange-correlation potential,

$$V_{\mathrm{xc},i}(\mathbf{r})=\epsilon_{\mathrm{xc}}(n_{\mathrm{tot},i}(\mathbf{r})) \quad (i=c,a) \tag{16}$$

where $n_{\mathrm{tot},i}$ is the total electronic density when the coordinates are chosen so that the system is centered on a type-i ion,

$$n_{\mathrm{tot},i}(\mathbf{r})=n_i(\mathbf{r})+\sum_{\mathbf{R}\neq 0} n_{\mathbf{R}}(\mathbf{r}-\mathbf{R}) , \tag{17}$$

and $\epsilon_{\mathrm{xc}}(n)$ is the exchange-correlation potential of a homogeneous electron gas of density n. For its calculation we have used the Perdew-Zunger parametrization of the Ceperley-Alder results.[10,19] Similarly, we make a local-density approximation for the kinetic-energy-correction potential,[14]

$$V_k(\mathbf{r})=(3\pi^2)^{2/3}\{[n_{\mathrm{tot},i}(\mathbf{r})]^{2/3}-[n_i(\mathbf{r})]^{2/3}\} , \tag{18}$$

where each term is the result for a homogeneous electron gas (in rydbergs). We are dealing here with closed-shell ions which in isolation are spherically symmetric and in the crystal are placed in centrosymmetric positions; thus our final practical approximation is to replace the total density in (16) and (18) with the spherical average of the density (17), and similarly to spherically average the other terms in (15). The significance of these latter two approximations is discussed below. We note that because of the spherical averaging we are able to compute only the diagonal terms of the hyperpolarizability tensors, although the anisotropy can be treated perturbatively.

Because of the spherical averaging, each term within large parentheses in (15) represents the potential due to a spherically symmetric charge distribution, centered on a point $\mathbf{R}$, of zero overall charge. Hence these terms are negligible unless there is significant overlap between the central electron cloud and the cloud centered on $\mathbf{R}$, and it is sufficient to keep one or at most two nearest-neighbor shells in the sums.

The self-consistent solution requires that we solve the coupled equations (11) for both a central anion and a central cation, and then substitute the densities n_a and n_c into V_{eff} [(15), (16), (18), approximated as above]. The process is repeated until self-consistency is achieved.

The total energy per pair in the crystal is

$$E=E_a+E_c+E_{\mathrm{Mad}} \tag{19}$$

with

$$E_i=\sum_{\alpha}\varepsilon_{i\alpha}-\int d^3r\int d^3r'\frac{n_i(\mathbf{r})n_i(\mathbf{r}')}{|\mathbf{r}-\mathbf{r}'|}+\int d^3r\, n_i(\mathbf{r})[\varepsilon_{\mathrm{xc},i}(\mathbf{r})-V_{\mathrm{xc},i}(\mathbf{r})-\tfrac{2}{5}V_{K,i}(\mathbf{r})]$$
$$-(Z_i-I_i)V_{\mathrm{Mad},i}(\mathbf{r}=0)-\sum_{\mathbf{R}\neq 0}\left[\int d^3r\int d^3r'\frac{n_i(\mathbf{r})n_{\mathbf{R}}(\mathbf{r}'-\mathbf{R})}{|\mathbf{r}-\mathbf{r}'|}-\frac{1}{R}(Z_i-I_i)(Z_{\mathbf{R}}-I_{\mathbf{R}})\right] , \tag{20}$$

$$E_{\mathrm{Mad}}=-\frac{2I_c^2}{a_{\mathrm{NN}}}\alpha_{\mathrm{Mad}} , \tag{21}$$

where the exchange-correlation energy density of a homogeneous electron gas is $n\varepsilon_{\mathrm{xc}}(n)$ and $\varepsilon_{\mathrm{xc},i}(\mathbf{r})=\varepsilon_{\mathrm{xc}}(n_{\mathrm{tot},i}(\mathbf{r}))$. E_{Mad} is the Madelung energy per pair (in rydbergs); a_{NN} is the nearest-neighbor distance in the crystal (in Bohr radii), and α_{Mad} is the Madelung constant (1.747 565 for the NaCl structure). The term within large parentheses vanishes for distant ions.

B. Pseudopotential method

This approach was used by Mahan to compute the linear dipole polarizability,[16] and is easily extended to the calculation of hyperpolarizabilities. The interaction of an ion with other ions is replaced by an external potential constructed from pseudopotentials, and the cation and anion problems decouple. Interactions among electrons belonging to the central ion are required to be self-consistent, so this method could be called partially self-consistent, in contrast to the completely self-consistent method described in the preceding section.

Here, the cation's effective potential [in contrast to (15) in the completely self-consistent case] is

$$\tilde{V}_{\mathrm{eff},c}(\mathbf{r})=2\int d^3r'\frac{n_c(\mathbf{r}')}{|\mathbf{r}-\mathbf{r}'|}-\frac{2Z_c}{r}+\epsilon_{\mathrm{xc}}(n_c(\mathbf{r}))$$
$$+\sum_{\substack{\mathbf{R}\neq 0\\ \text{cations}}}V_{\mathrm{pseudo},c}(\mathbf{r}-\mathbf{R})$$
$$+\sum_{\substack{\mathbf{R}\\ \text{anions}}}V_{\mathrm{pseudo},a}(\mathbf{r}-\mathbf{R}) \tag{22}$$

with a similar expression for the anion. For the cations we use Heine-Aberenkov pseudopotentials

$$V_{\mathrm{pseudo},c}(r)=\begin{cases}-2/r, & r>r_i\\ A_i, & r<r_i\end{cases} \tag{23}$$

with published values for the parameters.[15] For the anions, following Mahan, we arbitrarily add a constant

of 0.1 Ry at the Pauling radius of the ion,[20]

$$V_{\text{pseudo},a}(r)=\begin{cases}2/r, & r>r_i\\ 2/r+A, & r<r_i\end{cases}. \tag{24}$$

The results are weakly sensitive to the value of A; the value $A=0.1$ Ry gives a good match to the experimental linear polarizabilities for the alkali halides.

In practice we used the pseudopotentials only for the nearest four neighboring shells, with more distant ions contributing only a Madelung potential; the effective potential (22) was then spherically averaged. The calculation then proceeds self-consistently, in a manner formally identical to placing an atom (or ion) in an arbitrary external potential.

C. Computing linear and nonlinear polarizabilities

The static linear and nonlinear polarizabilities can be computed using a self-consistent Sternheimer approach. This method was first used to compute the static linear polarizability (in the pseudopotential approximation),[15,16] and has been extended to complete self-consistency (as in Sec. II A above) and nonlinear polarizabilities.[14,4] We refer to the latter[4] for details of the calculation. In this section we describe how the method can be used to compute polarizabilities in the crystal.

In what follows, we deal with "in-crystal" polarizabilities describing the response of the ions to the local field resulting from an applied external field. Because of the localized character of the charge distribution in these ionic crystals, we relate the in-crystal polarizabilities to the macroscopic quantities via the Clausius-Mossotti relation (for the linear polarizability) and its generalizations[1] (for nonlinear polarizabilities). Note that the use of such relations amounts to taking account of dipole-induced-dipole (DID) effects at the level of a point-dipole description.

When an ion in the crystal is placed in a static local electric field $\mathbf{F}=F\hat{\mathbf{z}}$, the ion feels a (bare) perturbing potential

$$V=fr\cos\theta\ , \tag{25}$$

where $f=F/F_0$, $F_0=e/(2a_0^2)$. This perturbation changes the Kohn-Sham orbitals and hence the ground-state electronic density and energy from the zero-field values calculated as in Secs. II A and II B. The perturbed quantities can be expanded in powers of f, e.g.,

$$n_i=n_i^{(0)}+fn_i^{(1)}+f^2n_i^{(2)}+f^3n_i^{(3)}+\cdots\quad(i=a,c)\ . \tag{26}$$

It is then evident from (15) and (22) that the effective potentials will also gain perturbing terms to all orders in f:

$$V_{\text{eff},i}=V_{\text{eff},i}^{(0)}+fV_i^{(1)}+f^2V_i^{(2)}+f^3V_i^{(3)}+\cdots\ , \tag{27}$$

as can be seen by expanding the density. Thus in a self-consistent perturbative calculation (based on either zero-field method), rather than simply the bare perturbation (25), there are in effect perturbing potentials to all orders in f. By expanding the Kohn-Sham equations (11), one finds that there is a hierarchy of equations to be solved sequentially.[4] The polarizabilities can be written

$$\alpha=-\int d^3r\,n^{(1)}(\mathbf{r})r\cos\theta\ , \tag{28}$$

$$B=-6\int d^3r\,n^{(2)}(\mathbf{r})r^2P_2(\cos\theta)\ , \tag{29}$$

$$\gamma/6=-\int d^3r\,n^{(3)}(\mathbf{r})r\cos\theta\ , \tag{30}$$

in units of $2a_0^3$, $4a_0^6/e$, and $8a_0^7/e^2$, respectively, where we have written $\gamma_{zzzz}\equiv\gamma$ and $B_{zzzz}\equiv B$.

We carry over the practical approximations made in the zero-field calculation, plus one other: a central ion's neighbors are held frozen when the field is switched on, which neglects any dipole-induced-dipole contributions beyond those of the point dipoles already embodied in the use of the Clausius-Mossotti relation and its generalizations. The effects of this neglect and of the spherical averaging are discussed below. For the pseudopotential calculation, the perturbed potentials can be written

$$\tilde{V}_i^{(j)}=\delta_{j1}r\cos\theta+2\int d^3r'\frac{n_i^{(j)}(\mathbf{r}')}{|\mathbf{r}-\mathbf{r}'|}+\tilde{V}_{\text{xc},i}^{(j)}(\mathbf{r})\quad(i=c,a)\ , \tag{31}$$

where $\tilde{V}_{\text{xc}}^{(j)}$ comes from expanding $\epsilon_{\text{xc}}(n_i(\mathbf{r}))$ in powers of f.[4] In the self-consistent calculation, since the neighboring ions are frozen,

$$n_{\text{tot},i}=n_{\text{tot},i}^{(0)}+fn_i^{(1)}+f^2n_i^{(2)}+f^3n_i^{(3)}+\cdots \tag{32}$$

and

$$V_i^{(j)}(\mathbf{r})=\delta_{j1}r\cos\theta+2\int d^3r'\frac{n_i^{(j)}(\mathbf{r}')}{|\mathbf{r}-\mathbf{r}'|}+V_{\text{xc},i}^{(j)}(\mathbf{r})+V_{K,i}^{(j)}(\mathbf{r})\ . \tag{33}$$

Note that here the neighboring ions are frozen (i.e., in (32), $n_i^{(j)}$ is the jth-order induced density of the central ion only). $V_{K,i}$ comes from expanding (18),

$$V_{K,i}^{(1)}(\mathbf{r})=\tfrac{2}{3}(3\pi^2)^{2/3}[(n_{\text{tot},i}^{(0)})^{-1/3}-(n_i^{(0)})^{-1/3}]n_i^{(1)}(\mathbf{r})\ , \tag{34}$$

etc. With these approximations the polarizability calculation follows very much like that of the free ion.[4]

Next we consider the consequences of spherical averaging and of freezing the density of neighboring ions. In the case of an isolated closed-shell ion in a static electric field, the induced charge densities (26) can be expanded in Legendre polynomials:[4]

$$n_i^{(j)}(\mathbf{r})=\sum_l n_{il}^{(j)}(\mathbf{r})P_l(\cos\theta)\ . \tag{35}$$

The zero-field density $n_i^{(0)}$ in this case has only an $l=0$ component (spherical symmetry). Higher-order terms in the density are sums over only a few values of l. These can be found by a kind of angular momentum addition: the bare perturbation (25) goes as $P_1(\cos\theta)$ (i.e., is an $l=1$ term); this adds to the $l=0$ density $n_i^{(0)}$ to give an $l=1$ first-order density $n_i^{(1)}$, and then adds again to the latter to give both $l=0$ and $l=2$ components for $n_i^{(2)}$, and so $l=1$ and $l=3$ components for $n_i^{(3)}$. These indi-

cative statements can, in fact, be proven rigorously for the isolated closed-shell ion, including the self-consistent perturbation terms of (27).[4]

Next we turn to the situation in a cubic crystal. The Sternheimer scheme sketched above works simply in the case of isolated closed-shell ions because of their spherical symmetry. However, for an ion in a crystal there are two complications: the exact zero-field density $n_i^{(0)}$ is of course not spherically symmetric; and additionally, in the self-consistent calculation, an electric field perturbs not just the central ion but neighboring ions as well. However, by treating the crystal potential in a perturbative or recursive way, we can show that neither of these alters the linear polarizability α_i, and as far as its calculation is concerned both complications can be neglected.

Consider first the zero-field situation, and focus on the electrostatic (Hartree) potential coming from electrons on neighboring ions (or equally well consider pseudopotentials centered on these sites). In the zero-field state, spherically averaging this crystal potential gives only the $l=0$ component of $n_i^{(0)}$. If these spherically symmetric densities (or pseudopotentials) are then placed on cubic sites, they contribute components with $l=0$ and $l\geq 4$ (even) to the potential felt by the central ion. Hence in a cubic crystal $n_i^{(0)}$ will have a spherically symmetric ($l=0$) component plus $l=4$ terms (actually spherical harmonics Y_4^m), as well as higher-l pieces.

If an electric field is then switched on, the first-order-induced density $n_i^{(1)}$ will have an $l=1$ component coming from adding the $l=1$ perturbation to the $l=0$ piece of $n_i^{(0)}$, plus $l=3,5$, etc., components from the $l=4$ and higher pieces of $n_i^{(0)}$. In the self-consistent calculation, moreover, placing the induced densities $n_{il}^{(1)}$ (with $l=1,3,5$, etc., pieces) back on sites of cubic symmetry adds to the central ion's potential only terms with $l\geq 3$. Hence the $l=1$ component of $n_i^{(1)}$ comes only from the spherically symmetric ($l=0$) piece of $n_i^{(0)}$, and is not changed by either higher-l pieces in the zero-field cubic density, or by self-consistently including induced neighbors. Since the linear polarizability α depends only on this $l=1$ piece of $n_i^{(1)}$ [see (28)], the cubic fields and induced neighbors can be neglected in computing α_i.

This argument cannot be extended to the nonlinear polarizabilities. For example, the dipole hyperpolarizability γ_i depends on the $l=1$ component of $n_i^{(3)}$ [see (30)]. Following a sequence as above, this term comes from the $l=0$ and $l=2$ components of $n_i^{(2)}$, which in turn arise from the $l=1$ and $l=3$ pieces of $n_i^{(1)}$, which depend on the $l=0$ and $l=4$ components of $n_i^{(0)}$. Nevertheless, we expect the dominant contribution to the hyperpolarizability to come from distortions of the central ion's $l=0$ zero-field density, and so we spherically average the crystal potential and (in the self-consistent calculation) freeze neighboring ions. In the pseudopotential approach this turns out to be quite accurate—it neglects only a small $l=4$ contribution to the zero-field state. In the self-consistent calculation the picture is more complicated—for instance, the $l=1$ part of $n_i^{(1)}$ feeds back, when placed on neighboring sites, to change the $l=1$ density in third order. Freezing the neighboring ions neglects these dipole-induced-dipole contributions (and similar $l=0$ contributions), and is accurate only to the extent that the higher-order-induced density does not extend significantly into the overlap region. Some of the formal aspects of these local-field corrections have been considered by Mahan and Subbaswamy.[21]

III. RESULTS AND DISCUSSION

A. Effects of the crystalline environment

We have calculated the static linear polarizability $\alpha^{\pm}$ and the dipole and quadrupole hyperpolarizabilities $\gamma^{\pm}$ and $B^{\pm}$ using both methods described above, for all of the alkali halides with the rocksalt structure. Before turning to these results, we begin this section with a detailed discussion of the calculation in one test case, KCl. There are two points, in particular, to emphasize—the consequences of electron-electron overlap in the crystal, and the range of validity of the pseudopotential and self-consistent calculations.

Table I shows the polarizabilities of the cation K^+ and the anion Cl^- in several situations. In the first line of Table I the polarizabilities of an isolated K^+ cation are included for comparison with the in-crystal results. (The free anion is not shown because in the absence of self-interaction corrections, which we neglect, the isolated anion does not bind.) The second line shows the polarizabilities of the (decoupled) K^+ and Cl^- ions placed in a crystal of fixed point charges; i.e., in this calculation the crystal potential is simply the Madelung potential (14). The third and fourth lines are the results for the complete self-consistent calculation. The results in the third line were obtained by including (besides the Madelung contribution from more distant ions) the over-

TABLE I. Calculated linear and nonlinear static polarizabilities of KCl.

	α (10^{-24} esu)		$\gamma/6$ (10^{-39} esu)		B (10^{-40} esu)	
	(+)	(−)	(+)	(−)	(+)	(−)
Free ion	0.850		11.3		14.4	
Madelung only	0.850	5.01	11.8	1810	14.5	881
Self-consistent, nearest-neighbor shell	0.848	3.39	11.0	362	14.2	267
Self-consistent, two neighboring shells	0.847	3.36	11.0	293	14.2	247
Pseudopotential, nearest-neighbor shell	0.838	3.55	10.6	564	13.7	339
Pseudopotential, two neighboring shells	0.838	3.50	10.4	487	13.6	317

lap of the ion with its nearest neighbors in the crystal; i.e., in the sums in (15) only the nearest-ion shell was retained. In the fourth line both nearest and next-nearest neighbors were included. Similarly, the fifth and sixth lines are the polarizabilities calculated using the pseudopotential approach, including first-neighbor and first- and second-neighbor shells, respectively.

The first point to note from Table I is that the polarizabilities—linear and nonlinear—of the cation are essentially unchanged when it is placed in the crystal, while the polarizabilities of the anion depend strongly on its local environment.[15,9] The cation is quite tightly bound, and surrounding one by a shell of point charges changes its electronic density only slightly. For example, surrounding a free K^+ by a lattice of point charges (the Madelung potential) increases γ^+ and B^+ slightly (first and second lines of Table I), reflecting the expected small expansion of the cation's electron cloud.

When electrons are included on the nearest-neighbor shell or two of the ions (rather than treating them as point charges), electron-electron overlap repulsion compresses the central ion's electron cloud, leading to a decrease in its polarizabilities. This can be seen in the change (cf. the second and third lines of Table I) that results when overlap with only the nearest-neighbor shell is included. The cation's polarizabilities are only slightly diminished, but the effect on the anion is quite dramatic. In KCl, the anion's linear polarizability α^- decreases by 32%, and the hyperpolarizability γ^- drops by a factor of 5. These large decreases arise because the electrons are very loosely bound on the negatively-charged anions, and the addition of overlap repulsion substantially increases their binding. The pseudopotential calculation reproduces this overlap effect by adding a core repulsion term [A_i in (23) or (24)]; and, in fact, behavior quite similar to the self-consistent results is seen in going from the Madelung-only case to a single nearest-neighbor shell of pseudopotentials (cf. the second and fifth lines in Table I).

Quantitatively, the self-consistent and pseudopotential calculations agree fairly well for the cation but less so for the anion—understandably, since the anion is far more sensitive to its local environment. The anion's polarizabilities computed with the self-consistent approach are smaller than those computed using pseudopotentials; when one nearest-neighbor shell is included, the difference is small for α^- (4%), but much larger for the hyperpolarizabilities (36% for γ^- and 21% for B^-). A clue to the reason for the large difference in the hyperpolarizabilities is given by adding in the next-nearest neighbors in the crystal (the fourth and sixth lines of Table I). These tend to change the tail region of the central ion's electronic cloud. From Table I we see that including next-nearest neighbors changes α^- only slightly (1%), but γ^- changes much more (19% and 14%, respectively, for the self-consistent and pseudopotential calculations). Thus the hyperpolarizability is much more sensitive than is the linear polarizability to the tail of the electronic cloud, which is to say the region of overlap.

The density in the tail region depends on the details of the crystal potential used, which is where the two approaches differ. In Fig. 1 we have plotted the spherically averaged zero-field crystal potential felt by Cl^- in KCl for both the self-consistent and pseudopotential methods (the former with one nearest-neighbor shell, the latter with four). The crystal potential is $V_{\rm eff}$ with the central ion's contributions subtracted off. The peak in the self-consistent crystal potential represents overlap repulsion; its large size can be traced to the LDA approximation (18) for V_K. The large repulsion exaggerates the degree of confinement felt by the anion, reducing the electronic density in the tail region and hence the hyperpolarizability. The fact that (18) gives an excessive overlap repulsion is more clearly seen in other alkali halides besides KCl; in LiF, for example, adding next-nearest neighbors in the pseudopotential calculation reduces γ^- by a reasonable 22%, while in the self-consistent calculation the decrease is a physically unrealistic 64%.

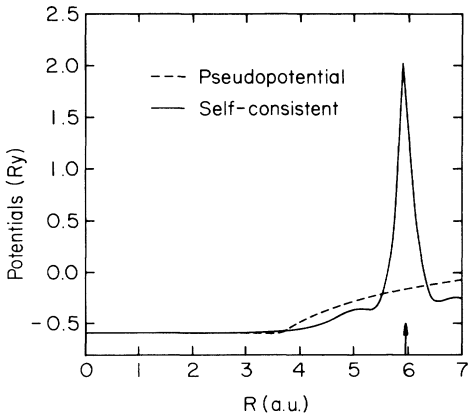

FIG. 1. Crystal potential of Cl^- in KCl. The crystal potential is $V_{{\rm eff},a}$ minus the contribution from the central Cl^- ion. (The arrow marks the location of the nearest K^+ shell.)

This limits the range of validity of the self-consistent approach. The linear polarizabilities are dominated by induced distortions in relatively central regions of an ion's electron cloud, with a small contribution from distortions in the overlap region. Both the self-consistent and pseudopotential approaches represent this region (the bulk of the electronic density) well, and give similar results for the linear polarizability. However, the hyperpolarizabilities depend more on induced distortions in the tail or overlap region; in the self-consistent calculation the density tail, and hence the hyperpolarizabilities, are artificially reduced by the excessive overlap repulsion given by the LDA approximation (18) for V_K. As a consequence, we have used both approaches to calculate the linear polarizability, but only the pseudopotential method for the hyperpolarizabilities.

B. Linear polarizability

In Table II we show the calculated and experimental linear polarizabilities of the alkali halides with the rock-salt structure. The self-consistent calculation was carried through retaining next-nearest neighbors in the crystal, while in the pseudopotential calculation pseudo-

TABLE II. Calculated and experimental static linear polarizabilities α of alkali halides (all values in 10^{-24} esu).

	Self-consistent			Pseudopotential[a]			Experiment[b]
	α^+	α^-	$\alpha^+ + \alpha^-$	α^+	α^-	$\alpha^+ + \alpha^-$	α_{tot}
LiF	0.031	0.948	0.979	0.032	0.848	0.880	0.91
LiCl	0.032	3.19	3.22	0.032	2.81	2.84	2.94
LiBr	0.032	4.31	4.34	0.032	3.86	3.89	4.09
LiI	0.032	6.48	6.51	0.032	5.67	5.70	6.33
NaF	0.155	0.938	1.09	0.158	1.13	1.29	1.17
NaCl	0.159	2.89	3.05	0.158	3.26	3.42	3.24
NaBr	0.160	3.92	4.08	0.158	4.40	4.56	4.38
NaI	0.160	5.81	5.97	0.159	6.37	6.53	6.63
KF	0.821	1.21	2.03	0.839	1.28	2.12	1.98
KCl	0.847	3.36	4.21	0.838	3.50	4.34	4.15
KBr	0.849	4.44	5.29	0.838	4.66	5.50	5.29
KI	0.855	6.45	7.31	0.838	6.68	7.52	7.56
RbF	1.35	1.22	2.57	1.39	1.38	2.77	2.49
RbCl	1.40	3.34	4.74	1.39	3.68	5.07	4.78
RbBr	1.40	4.43	5.83	1.39	4.89	6.28	5.96
RbI	1.42	6.32	7.74	1.38	6.95	8.33	8.25

[a]Calculation follows Ref. 16.
[b]From refractive index data of Lowndes and Martin (Refs. 22 and 16).

potentials were used out to fourth-nearest neighbors; in both cases, more distant ions were represented by their point charge (Madelung) contributions. (The pseudopotential calculation of α is taken from Refs. 15 and 16.) As in the KCl example above, a cation is essentially unaffected by its environment (here meaning the anion with which it is paired), while each anion's polarizability varies considerably as it is paired with different cations.

In the pseudopotential calculation, a particular anion's linear polarizability is seen from Table II to grow monotonically with the size of its cation partner (i.e., as it is paired with Li^+, Na^+, K^+, Rb^+), or equivalently as the lattice spacing grows.[15] This trend is intrinsic in the form of the pseudopotential: the crystal potential confining an anion's electrons is broad (Fig. 1); its effect is determined by the distance from the central ion to the edge of its neighboring cation's core repulsion (nearest-neighbor distance minus the cation's Pauling radius r_i) and the strength of the repulsion (A_i). For a given anion, the former is nearly a constant, equal to the anion's Pauling radius. Hence the upward trend in α^- is determined by the size of the cation's core repulsion A_i, which decrease monotonically as the cation's size (and so the lattice spacing) increases.

There is no such *a priori* reason for the self-consistent calculation to show such a trend in α^-, and in fact it does not. As an anion is paired with cations of increasing size, the lattice spacing grows, but the nearest electrons belonging to the cation remain at a distance of (approximately) the anion's Pauling radius. The linear polarizability represents a competition between two overlap effects—the greater distance to a neighboring cation's core electrons as the cation's size grows, which tends to increase α^-, and the greater total number of electrons on the cation, which tends to decrease α^-.

Both the self-consistent and pseudopotential approaches agree quite well with experiment[16,22] (see Table II), with discrepancies ranging up to 10% and an average disagreement of about 4%. These results are also shown in Fig. 2, where we have plotted the total polarizability per cation-anion pair against nearest-neighbor spacing. The increase in $\alpha^+ + \alpha^-$ (for a particular anion) with lattice constant is largely a consequence of the increasing cation polarizability α^+.

C. Hyperpolarizabilities

Table III shows the hyperpolarizabilities γ and B calculated using four nearest-neighbor pseudopotential shells (with point charges for more distant ions). As dis-

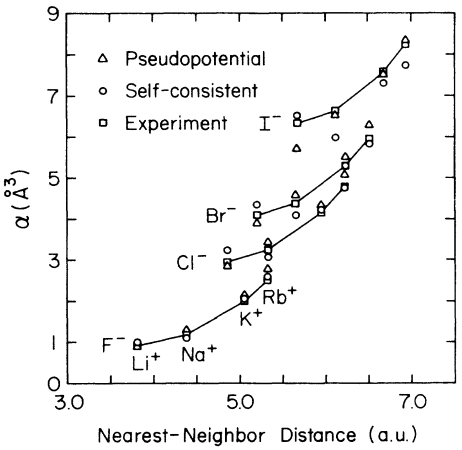

FIG. 2. Linear polarizabilities $\alpha^+ + \alpha^-$ of alkali halides. Line segments connect measured values [from the refractive index data of Lowndes and Martin (Ref. 22)].

TABLE III. Calculated static dipole and quadrupole hyperpolarizabilities of alkali halides, computed using pseudopotentials.

	$\gamma/6$ (10^{-39} esu)		B (10^{-40} esu)	
	(+)	(−)	(+)	(−)
LiF	0.029	40.6	0.073	29.5
LiCl	0.029	201	0.074	167
LiBr	0.029	339	0.074	282
LiI	0.029	630	0.074	528
NaF	0.602	86.3	1.01	57.9
NaCl	0.593	339	1.00	252
NaBr	0.593	538	1.00	405
NaI	0.593	965	1.00	731
KF	10.4	130	13.6	80.1
KCl	10.4	459	13.6	312
KBr	10.3	698	13.5	483
KI	10.2	1210	13.5	850
RbF	29.0	169	34.0	97.9
RbCl	29.0	574	33.9	364
RbBr	28.7	870	33.8	562
RbI	28.4	1470	33.7	966

TABLE IV. Measured nonlinear susceptibility $\chi^{(3)}_{zzzz}$ of alkali halide crystals (in 10^{-14} esu).

	$\chi^{(3)}_{zzzz}$ (10^{-14} esu)		
	THG[a] (±300%)	FWM (±20%)	NRI[f] (±50%)
LiF	0.4	0.2[b]	0.9
		0.34[c]	
LiCl		0.6[d]	
NaF	0.4		0.33
NaCl	1.7	1.3[e]	2.63
NaBr			4.13
KF		0.14[d]	
KCl	1.7	1.9[b]	1.30
KBr	3.9	3.0[b]	5.83
KI		4.4[e]	4.88
		3.6[d]	

[a]Reference 23, $\lambda=1.06$ μm.
[b]Reference 25, $\lambda_1=0.6943$ μm, $\lambda_2=0.7457$ μm.
[c]Reference 26, $\lambda_1=0.6943$ μm, $\lambda_2=0.7457$ μm.
[d]Reference 27, $\lambda_1=1.06$ μm, $\lambda_2=0.527$ μm.
[e]Corrected values from measurements in Reference 25, as cited in Ref. 24.
[f]Reference 28, $\lambda=1.06$ μm.

cussed in detail above, the pseudopotential calculation of hyperpolarizabilities is much more reliable than the self-consistent approach; for the Li^+ compounds the two approaches agree fairly well, but in the remaining compounds the self-consistent approach underestimates by about 50% the more accurate pseudopotential result. Table III presents the hyperpolarizabilities computed using the pseudopotential approach.

Both trends evident in the linear polarizabilities can also be seen in the pseudopotential calculation of hyperpolarizabilities. First, a cation's hyperpolarizabilities are largely independent of the crystal environment and hence do not change as a cation is paired with different anions. Second, an anion's hyperpolarizabilities γ^- and B^- increase monotonically with the lattice constant, for the same reason given above for the linear case. In fact, the increase is much more marked for hyperpolarizabilities: γ^- increases by a factor of 3 or 4 when Li^+ is replaced by Rb^+, while α^- increased by only 20–60%. Additionally, even more than in the case of the linear polarizability, the total dipole hyperpolarizability $\gamma^+ + \gamma^-$ per ion pair is dominated by the anion's contribution.

IV. COMPARISON WITH HYPERPOLARIZABILITY MEASUREMENTS

Since the experimental measurements of the nonlinear susceptibilities of alkali halides are rather scarce, we begin with a brief survey of the reported measurements. The techniques used are as follows:[3] (1) third harmonic generation (THG), which measures $\chi^{(3)}(-3\omega;\omega,\omega,\omega)$; (2) four-wave mixing (FWM), which measures $\chi^{(3)}(-2\omega_1+\omega_2;\omega_1,\omega_1,-\omega_2)$; and (3) nonlinear refractive index (NRI) measurements, which give $\chi^{(3)}(-\omega;\omega,\omega,-\omega)$. The measured values[23–28] are collected in Table IV, along with cited uncertainties. One sees fair agreement between reported values. For purposes of comparison with our calculated values we shall use the FWM results listed in column three of Table IV.

We need to extrapolate the experimental numbers to the static values $\chi^{(3)}(0;0;0;0)$ for comparison with our calculated results. For this purpose we use the semiempirical formula[29,30]

$$\chi^{(3)}(\omega_4;\omega_1,\omega_2,\omega_3)=\chi^{(3)}(0;0,0,0)(1+c\omega_L^2/\omega_0^2)\ , \tag{36}$$

where ω_0 is determined from the dispersion of the linear susceptibility,

TABLE V. Comparison of pseudopotential LDA hyperpolarizability $\gamma^+ + \gamma^-$ with experimental values and other calculations. All numbers are in 10^{-39} esu.

	γ_{zzzz} (10^{-39} esu)		
	Expt.	LDA	FM[d]
LiF	404[a]	244	105
LiCl		1206	1050
NaF	772[b]	521	
NaCl	2520[a]	2038	
KCl	5831[a]	2816	
KBr	7912[a]	4250	
KI	8864[c]	7321	

[a]Extrapolated from measurements in Ref. 25.
[b]Extrapolated from measurements in Ref. 23.
[c]Extrapolated from corrected value cited in Ref. 24 of the measurements in Ref. 25.
[d]Fowler and Madden (Ref. 9).

$$\chi^{(1)}(\omega)=\chi^{(1)}(0)(1+\omega^2/\omega_0^2) , \quad (37)$$

and c is a number of order 10. The work on rare gases suggests[30] that we take $c \approx 3$. In the above $\omega_L^2=\omega_1^2+\omega_2^2+\omega_3^2+\omega_4^2$. To determine ω_0 we have used the refractive index dispersion data of Lowndes and Martin.[22] We note in passing that the ω_0 obtained in this way scale reasonably well with the first optical absorption peaks[31] in these crystals. From the extrapolated static values of $\chi^{(3)}$ we have inferred the experimental values for the static hyperpolarizabilities γ for the alkali halides via the relation[32]

$$\gamma=\frac{24V_0\chi^{(3)}}{\mathcal{L}^4} , \quad (38)$$

where V_0 is the volume of the primitive unit cell, and $\mathcal{L}=(\epsilon_\infty+2)/3$, with ϵ_∞ the optical-frequency dielectric constant. We compare this γ with the computed $\gamma^+ + \gamma^-$ in Table V. The extrapolated experimental results are listed in column two of Table V along with our calculated values in column one. The agreement is quite good, considering the known accuracy of both the experimental and theoretical values.

The only other first-principles theoretical calculation is that of Fowler and Madden[9] for LiF and LiCl by quantum chemical methods. In Table V we also compare our results with theirs. Fowler and Madden have shown that for free atoms and ions their calculation is quite reliable; however, they represent the neighbors by a truncated basis set, and also restrict to nearest neighbors, which should be a poor approximation for Li^+ compounds (for which the very small Li^+ ions only provide a portion of the cage confining an anion). Nonetheless, the two calculations are consistent.

V. SUMMARY

We have computed the static hyperpolarizabilities of alkali halide crystals with a local-density-approximation scheme. This represents the first extensive calculation for this important class of materials. The scheme is an extension of the highly successful linear polarizability computation using pseudopotentials to represent the crystalline environment. We have also tried a totally *ab initio* scheme which might be useful when no suitable pseudopotentials are available. This scheme, while yielding linear polarizabilities of the same quality as the pseudopotential scheme, underestimates the nonlinear susceptibilities considerably. This failure is attributed to the way the kinetic energy due to electron overlap is handled.

The computed hyperpolarizabilities show several trends. The cation susceptibilities are quite insensitive to the environment. The anion values, on the other hand, are highly sensitive to the environment. The hyperpolarizability of a given anion increases smoothly with the size of the cation by which it is surrounded. The computed values are in good agreement with the extrapolated experimental static values, considering the known accuracy of the experiments and the extrapolation procedure. There is need for more extensive, more reliable data, as well as information on the dispersion of the nonlinear susceptibilities.

ACKNOWLEDGMENTS

We acknowledge a helpful discussion with Dr. Lloyd Chase. This work was supported in part by the National Science Foundation (NSF) under Grant No. DMR82-16212. We also acknowledge a grant of computer time at the Pittsburgh Supercomputer Center through the Division of Advanced Scientific Computing of the NSF, and partial financial support from the University of Kentucky Center for Computational Sciences.

[1]N. Bloembergen, *Nonlinear Optics* (Benjamin, New York, 1965).
[2]H. Vogt, in *Light Scattering in Solids*, edited by M. Cardona and G. Guntherodt (Springer-Verlag, Berlin, 1986), Vol. 2, p. 207.
[3]See, e.g., R. W. Hellwarth, Prog. Quantum Electron. **5**, 1 (1977).
[4]G. Senatore and K. R. Subbaswamy, Phys. Rev. A **34**, 3619 (1986).
[5]G. Senatore and K. R. Subbaswamy, Phys. Rev. A **35**, 2440 (1987).
[6]I. Cernusak, G. H. F. Diercksen, and A. J. Sadlej, Phys. Rev. A **33**, 814 (1986).
[7]B. F. Levine, Phys. Rev. Lett. **25**, 440 (1970).
[8]S. Baroni and R. Resta, Phys. Rev. B **33**, 5969 (1986).
[9]P. W. Fowler and P. A. Madden, Phys. Rev. B **30**, 6131 (1984).
[10]J. Perdew and A. Zunger, Phys. Rev. B **23**, 5048 (1981).
[11]H. B. Shore, J. H. Rose, and E. Zaremba, Phys. Rev. B **15**, 2858 (1977).
[12]H. J. F. Jansen and A. J. Freeman, Phys. Rev. B **33**, 8629 (1986).
[13]A. D. Buckingham, Adv. Chem. Phys. **12**, 107 (1967).
[14]G. Senatore and K. R. Subbaswamy, Phys. Rev. B **34**, 5754 (1986).
[15]G. D. Mahan, Solid State Ion. **1**, 29 (1980).
[16]G. D. Mahan, Phys. Rev. B **34**, 4235 (1986).
[17]W. Kohn and L. J. Sham, Phys. Rev. **140**, A1133 (1965).
[18]P. Hohenberg and W. Kohn, Phys. Rev. **136**, B864 (1964).
[19]D. M. Ceperly and B. J. Alder, Phys. Rev. Lett. **45**, 566 (1980).
[20]This is a correction of Ref. 15.
[21]G. D. Mahan and K. R. Subbaswamy, Phys. Rev. B **33**, 8657 (1986).
[22]R. P. Lowndes and D. H. Martin, Proc. R. Soc. London, Ser. A **308**, 473 (1969).
[23]C. C. Wang and E. L. Baardsen, Phys. Rev. **185**, 1079 (1969); Phys. Rev. B **1**, 2827 (1970). The values were multiplied by 1.4 as indicated in Ref. 24 to account for normalization to He standard.

[24]C. C. Wang, Phys. Rev. B **2**, 2045 (1970).
[25]P. D. Maker and R. W. Terhune, Phys. Rev. **137**, A801 (1965).
[26]M. D. Levenson and N. Bloembergen, Phys. Rev. B **10**, 4447 (1974).
[27]A. Penzkofer, J. Schmailzl, and H. Glas, Appl. Phys. B **29**, 37 (1982).
[28]W. L. Smith, J. H. Bechtel, and N. Bloembergen, Phys. Rev. B **12**, 706 (1975).
[29]D. S. Elliott and J. F. Ward, Mol. Phys. **51**, 45 (1984).
[30]V. Mizrahi and D. P. Shelton, Phys. Rev. Lett. **55**, 696 (1985).
[31]T. O. Woodruff, Solid State Commun. **46**, 139 (1983).
[32]*Nonlinear Optics,* Ref. 1, pp. 68 and 69.